Amniotic Membrane Scaffolds Support Organized Muscle Regeneration in A Murine Volumetric Muscle Defect Model

Mohamed Awad, MD*
David E. Kurlander, MD*
Vikas S. Kotha, MD*
Kevin Malone, MD†
Edward H. Davidson, MD*
Anand R. Kumar, MD*

Background: Current treatment for volumetric muscle loss is limited to muscle transfer or acellular collagen scaffold (ACS) therapies that are associated with donor site morbidity and nonfunctional fibrosis, respectively. The aim of this study is to assess the utility of amniotic membrane scaffold (AMS) for volumetric muscle loss treatment.

Methods: Murine quadriceps defects were created and randomized to three groups (n = 5/group): untreated controls, ACS, and AMS. In vivo muscle regeneration volume was quantified by MRI and microcomputed tomography. Muscle explants were analyzed using standard histology and whole-mount immunofluorescence at 8 weeks.

Results: The cross-sectional muscle regeneration ratio was 0.64 ± 0.3 for AMS, 0.48 ± 0.07 for ACS, and 0.4 0 ± 0.03 for controls as assessed by MRI ($P = 0.09$) and 0.61 ± 0.28 for AMS, 0.50 ± 0.06 for ACS, and 0.43 ± 0.04 for controls as assessed by microcomputed tomography ($P = 0.2$). Histologically, AMS demonstrated significantly higher cellular density (900 ± 2 70 nuclei/high powered field) than ACS (210 ± 36) and control (130 ± 4) groups ($P = 0.05$). Immunofluorescence for laminin (AMS 623 ± 11 versus ACS 339 ± 3 versus control 115 ± 7; $P < 0.01$) and myosin heavy chain (AMS 509 ± 7 versus ACS 288 ± 5 versus control 84 ± 5; $P = 0.03$) indicated greater organized muscle fiber formation with AMS.

Conclusion: AMS mediated muscle healing was characterized by increased cellular infiltration and organized muscle formation when compared with controls and ACS. *(Plast Reconstr Surg Glob Open 2022;10:e4499; doi: 10.1097/GOX.0000000000004499; Published online 14 September 2022.)*

INTRODUCTION

Volumetric muscle loss (VML) treatment remains a significant reconstructive challenge. When spontaneous muscle regeneration is unattainable, wound healing with cicatrix formation occurs and tissue loss results in functional deficits and/or aesthetic deformities.[1,2] There remains an unmet need for treatment solutions that enhance muscle regeneration and minimize fibrotic healing seen after trauma, tumor resection, or muscle flap harvest. Current treatment options are limited to autologous muscle flaps and acellular scaffolds, which are associated with donor site morbidity and fibrosis, respectively, leading to permanent structural and functional deficits.[3,4] Engineered muscle grafts are a promising alternative to muscle flaps, but long-term tissue survival depends on rapid revascularization to meet the high metabolic demands of muscle.[5,6]

Recently, human amniotic tissue products have shown promising ability to promote wound healing. In vitro analyses have demonstrated a rich array of growth factors and cytokines native to these placental tissues known to facilitate wound healing.[7–14] Additionally, amniotic tissue products decrease inflammation and provide a scaffold for cellular ingrowth that may promote healing with minimal fibrosis.[7–14] In vivo murine studies have confirmed the bioactivity and efficacy of these factors after processing and storage. These growth factors and cytokines include platelet-derived growth factor-AA, platelet-derived growth factor-BB, transforming growth factor α, transforming growth factor β1, basic fibroblast growth

DOI: 10.1097/GOX.0000000000004499

Disclosure: *The authors have no financial interest to declare in relation to the content of this article.*

factor, epidermal growth factor, placental growth factor, granulocyte colony-stimulating factor, IL-4, 6, 8, and 10, and TIMP 1, 2, and 4.[7–14] Amniotic membrane matrices exhibit characteristics of an ideal scaffold and are acellular after harvest and processing by the manufacturer. Various extracellular proteins, including collagens, laminins, and fibronectins, may serve as an anchor for cell attachment and proliferation, while the local milieu of cytokines may promote tissue regeneration.[7–14]

Human studies have shown efficacy of amniotic tissue products in treatment of wound healing for diabetic foot ulcers, venous stasis ulcers, corneal ulcers, and tendon repair.[8–12,14–17,19,20] However, the ability of amniotic tissue products to heal a VML defect remains unknown. The aim of this study is to investigate the regenerative potential of an amniotic membrane umbilical cord (AMUC) scaffold to heal a VML defect in a murine quadriceps VML model previously developed and published by our group.[10–14] We hypothesize that an amniotic scaffold will lead to greater volume and quality of regenerated muscle compared with collagen scaffold and untreated controls.

MATERIALS AND METHODS

Murine Model of VML and Experimental Design

Case Western Reserve University Institutional Animal Care and Ethical Use Committee approval was obtained (2017-0143). Nude [forkhead box N1 (Foxn1) "J:NU"] (23±2 gram, 7–8 weeks old) female mice were commercially purchased from The Jackson Laboratory and used to create a VML defect model similar to a previously described murine VML defect model.[18] VML defect creation was performed under aseptic conditions. After induction of general anesthesia, a longitudinal incision was made over the right anterior thigh to identify the rectus femoris muscle. Next, a 5×5mm full-thickness muscle segment was excised, and 4-0 polypropylene suture was used to mark the cut ends of the muscle. After resection of the muscle segment and spontaneous retraction of the residual muscle, the AMS or ACS was placed into the residual defect with contact to each suture tail on opposite sides of the defect. The animals were divided into three groups (Table 1): (1) a control group with no additional treatment, (2) a group treated with 5×5mm collagen scaffold only (Gelfoam, Pfizer, New York, N.Y.) that was transplanted into the defect without any exogenous cellular elements, and (3) a group treated with 5×5mm amniotic membrane and umbilical cord–enriched collagen scaffolds (Amniox, Amniox Medical Inc., Miami, Fla.). After closure of the wound with 4-0 polypropylene suture and completion of surgery, all animals were monitored for recovery and wound healing. Animals were maintained under controlled room temperature conditions (22±1 °C at 60% ± 5% relative humidity), exposed to a 12-hour light/dark cycle, and fed with commercial standard pellets with free access to tap water.

Amniotic Membrane-umbilical Cord (AMUC)

Cryopreserved human amniotic membrane (AM) and umbilical cord (UC) tissue (Amniox, Amniox Medical

Takeaways

Question: What is the treatment for volumetric muscle loss?

Findings: This is a study in murine volumetric muscle loss defect model comparing acellular collagen scaffold (ACS) therapy and amniotic membrane scaffold (AMS) therapy as treatment options.

Meaning: AMS mediated muscle healing was characterized by increased cellular infiltration and organized muscle formation when compared with controls and ACS

Inc., Miami, Fla.) was processed by the CryoTek method (US 6,326,019, US 6,152,142, and PCT/US 2010/046675) by TissueTech, I 89 nc. (Miami, Fla.). To prepare cryopreserved AM and UC tissues, donated full-term human placentas with the umbilical cord were recovered after cesarean-section delivery, in compliance with American Association of Tissue Banks standards, and immediately stored at –80 °C for up to 12 months. Before processing, the frozen placenta and UC were thawed at room temperature for 8 hours in a Good Manufacturing Practice facility before being placed at 8 °C for an additional 16 hours. Under aseptic conditions, the placenta and UC were first cleaned of blood clots with phosphate-buffered saline (PBS) before separation of AM and UC by blunt dissection. The chorion was separated from the AM, and blood vessels were stripped from the UC to generate a flat graft before gentle rinsing in PBS until all blood colorations were removed. The AM was affixed on a filter membrane and cut to 6×6cm while the UC was cut to 6×3cm. The AM or UC tissue was then packaged in a pouch containing 1:1vol/vol Dulbecco Modified Eagle Medium and glycerol before storage at –80 °C. The AM was cut into slices of about 5×5mm immediately before transplant to the induced critical muscle defect.

Histologic Analysis

At the 8-week study endpoint, the entire right quadriceps muscle group was explanted for histologic analysis. Samples representing cross-sectional sections of regenerated muscle were processed for both permanent and frozen tissue embedding. Formalin-fixed and paraffin-embedded tissue was cut into 5-μm sections. Ten slides incorporating the muscle defect site of each animal were stained against hematoxylin and eosin (HE), and the cellular density per high-power field (10× hpf) was calculated using ImageJ. Whole-mount immunofluorescence was performed for select samples using a Zeiss 510 Meta laser scanning microscope (Carl Zeiss Microscopy, Jena, Germany). Immunofluorescence for myosin heavy chain (MyHC), 4′,6-diamidino-2-phenylindole (DAPI), and laminin was performed on unstained frozen sections. Tissue sections were fixed with 4% paraformaldehyde (Affymetrix, Inc., Santa Clara, Calif.) and permeabilized with Triton X-100 (Sigma-Aldrich 112 Corp., St. Louis, Mo.) in PBS. Blocking was performed using 1% bovine serum albumin (Sigma-Aldrich). The tissues were then incubated with either mouse anti-MyHC antibody (1:100; eBioscience)

Table 1. Animals Were Divided into Three Experimental Groups: Control Group, a Scaffold-only Group, Amniotic Membrane and Umbilical Cord–Enriched Collagen Scaffolds

Study Group	No. Subjects	Muscle Defect	Collagen Scaffold	Amniotic Scaffold	Time to Explantation
Control	5	Quadriceps	No	No	8 wk
Collagen scaffold	5	Quadriceps	Yes	No	8 wk
Amniotic scaffold	5	Quadriceps	No	Yes	8 wk

or rabbit antilaminin antibody (1:100; Abcam) at 4 °C overnight, followed by goat antimouse immunoglobulin G Alexa Fluor 596 (1:400; Life Technologies) or goat anti-rabbit immunoglobulin G Alexa Fluor 647 (1:400; Life Technologies) for 1 hour at room temperature. Finally, the tissues were counterstained with Hoechst 33342 nucleic acid stain (1:1000; Thermo Fisher Scientific, Waltham, Mass.). Image acquisition was performed with a Zeiss Axio Observer fluorescent microscope (Carl Zeiss Microscopy). Amira 2019.2 software used to quantify extend of fibrosis (Thermo Fisher Scientific, Waltham, Mass.). Fibrosis percentage was calculated using fluorescent stained slides of representative areas as follows: total area—area stained with my myosin and reported as percentage of muscle regenerated. Areas of interest selected in Amira using manual boundary selection.

Magnetic Resonance Imaging

At weeks zero, two, four, and eight, MRI studies were performed using a Bruker Biospec 7.0-T preclinical MRI scanner (Bruker Corp., Billerica, Mass.). Animals were anesthetized with isoflurane and placed in the prone position within a 7.0-T Bruker Biospec preclinical MRI scanner (Bruker, Billerica, Mass.). The respiratory rate (40–60 breaths/min) and core body temperature (35±1 °C) were monitored throughout the scanning session using an integrated animal-monitoring system (electrocardiograph, respiration, and body temperature) (SA Instruments, Stony Brook, N.Y.). High-resolution, T2W-MRI images in mm^3 were then acquired for each animal using a rapid MRI-acquisition technique (TR/TE = 7000 ms/70 ms, resolution = 400 µm × 400 µm, slice thickness = 1.5 mm, and two signal averages). Multiple signal averages and prospective respiratory gating were used to limit respiratory motion artifacts. Contiguous coronal, axial, and sagittal T2W images were acquired to ensure complete coverage of each animal's bilateral quadriceps muscle volume. All of the images were exported after MRI acquisition for offline 3D analysis of quadriceps regenerated volume using one-way analysis of variance of adjusted means in Amira 2019.2 and ImageJ.

Computed Tomographic Imaging

At the 8-week study endpoint, the animals were imaged using a carbon nanotube-based microcomputed tomography (mCT) system (GE Healthcare, Chicago, Ill.) to quantify muscle healing. Using the contralateral uninjured quadriceps as an internal comparison, the ratio of the cross-sectional area was obtained to control for variation between different animals. The cross-sectional area of the quadriceps muscle with the VML defect was calculated using Amira 2019.2 and ImageJ software.

Statistical Analysis

All values were reported as mean ± standard deviation, unless specified otherwise. Two-tailed unpaired *t* tests were used between group comparisons, where appropriate one-way analysis of variance was performed to determine significance using GraphPad Prism (Graphpad Software, Inc., La Jolla, Calif.). $P \leq 0.05$ was the threshold considered for statistical significance. To obtain adequate measurements, the number of animals/group was calculated as five mice per group. For all other animal cohorts, power analyses ($P = 0.05$, $\beta = 0.8$, SigmaStat, SPSS) utilized data from the least powerful outcome measure for each cohort. All measurements were performed by a trained research fellow.

RESULTS

MRI and Micro-CT Analysis

On MRI, the greater quadriceps cross-sectional area was seen in the amniotic scaffold (0.64±0.30) and collagen scaffold (0.48±0.07) groups compared with untreated controls (0.40±0.03; $P = 0.09$), although this did not reach significance. The amniotic scaffold group showed 25% greater muscle volume restoration than the collagen scaffold group and 60% greater muscle volume restoration than the control group, but this did not reach significance. On mCT, the amniotic scaffold group (0.61±0.28) did not have a significantly different quadriceps cross-sectional ratio compared with the collagen scaffold (0.50±0.06) and untreated control groups (0.43±0.04) ($P = 0.2$).

Gross and Cellular Evaluation

Clinical gross photographs were taken to evaluate tissue healing. The muscle defect in the untreated control group showed more fibrosis, as evidenced by formation of a dense fibrous band. In comparison, the collagen scaffold group appeared less fibrotic than in untreated controls. The amniotic scaffold group demonstrated the least amount of gross fibrosis (40% of regenerated muscle versus 60% in the collagen scaffold group versus 85% in the untreated control group) and had tissue quality that was most consistent with muscle regeneration. These observations were confirmed on HE-stained sections. The untreated control group exhibited significant fibrosis, as evidenced by dense collagen fiber deposition with minimal cellular components present. In contrast, the collagen scaffold and the amniotic scaffold groups had minimal fibrosis on histologic evaluation. The amniotic scaffold group also had a significantly higher cellular density (802±271 nuclei/hpf) compared with collagen scaffold (343±72 nuclei/hpf) and untreated control (160±80 nuclei/hpf) groups ($P < 0.01$).

Immunofluorescence Evaluation

To examine the quality of muscle healing, immunofluorescence of frozen sections of the explanted muscle was performed for DAPI (nuclear density), laminin (basement membrane protein), and MyHC (skeletal muscle protein). In the amniotic scaffold group, there was significant organized mature skeletal muscle formation. As represented by DAPI, the amniotic scaffold group (900±270 nuclei/hpf) demonstrated significantly higher cellular density compared with the collagen scaffold (210±36 nuclei/hpf) and untreated control groups (130±47 nuclei/hpf; $P = 0.05$). Immunofluorescence for laminin was 623±11 basement membrane protein/hpf for amniotic scaffold group, 339±3 basement membrane protein/hpf for collagen scaffold group, and 115±7 basement membrane protein/hpf for controls ($P < 0.01$). Immunofluorescence for MyHC was 509±7 MyHC/hpf for amniotic scaffold group versus 288±5 MyHC/hpf for collagen scaffold group versus 84±5 MyHC/hpf for controls ($P = 0.03$). Additionally, histological results from HE and immunohistochemistry suggest organized muscle fiber formation along the alignment of the native muscle fibers in the amniotic scaffold group. Merged immunofluorescence results are shown in Figure 1.

DISCUSSION

The purpose of this study was to assess the ability of an AMUC scaffold to promote healing of a VML defect. The findings demonstrate that an amniotic scaffold can promote greater volumetric muscle regeneration compared with collagen scaffold and untreated control groups with formation of organized muscle fibers, findings that were largely absent following collagen scaffold treatment and no treatment. Additionally, the regenerated muscle has greater formation of normal architecture and decreasing central gap with less fibrosis. These findings suggest that an amniotic scaffold may promote myogenesis while inhibiting collagen deposition and fibrosis in a manner similar to scar-less fetal wound healing. The proposed mechanism of regeneration would be through host progenitor cell repopulation, mediated by the favorable cytokine signaling inherent to the amniotic scaffold.[15,21–25] Amniotic scaffold may offer a potential therapeutic advantage for treating VML defects compared with currently available autologous treatments associated with donor site morbidity and acellular allograft scaffolds associated with fibrosis demonstrated in HE.

Many strategies for functional muscle regeneration have been described. Our group has previously published on muscle-derived stem cell–enriched scaffolds for VML healing.[26] In both strategies, host progenitor cells contribute significantly to myogenesis, likely via paracrine signaling from a variety of growth factors and direct cellular migration into the scaffolding material. An advantage of AMS is it is readily available in large quantities and does not require cellular expansion. AMUC tissue is recovered after cesarean-section delivery from placental tissues and processed using a cryopreservation protocol, so as to retain anti-inflammatory and antiscarring properties as well as structural components. The difference in efficacy between an autologous stem cell and allograft amniotic approach remains to be elucidated.
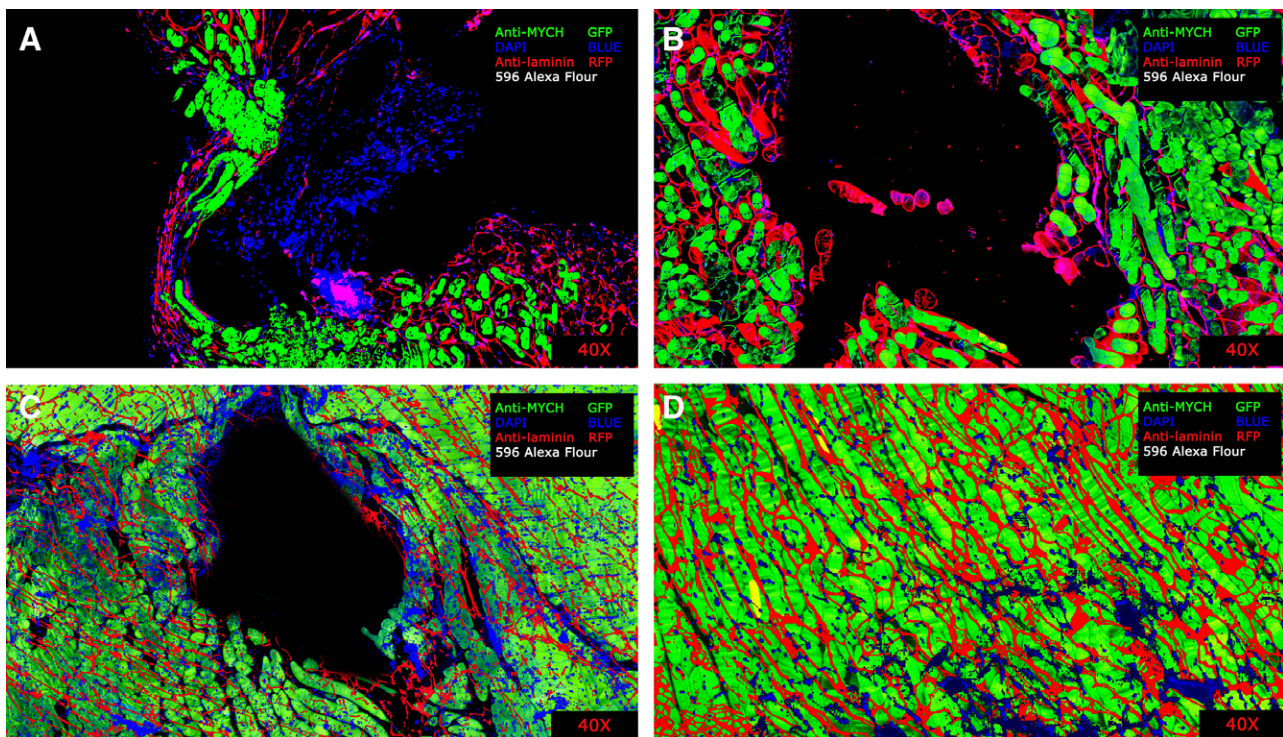
Fig. 1. Merged immunofluorescence for DAPI (blue), laminin (red), and MyHC (green). A, The control group. B, The collagen scaffold group. C, The amniotic scaffold group. D, Imaging of the contralateral uninjured healthy quadriceps are provided for comparison.

AMUC contains multiple extracellular matrix components, cytokines, growth factors, and proteins. Heavy chain 1-hyaluronic acid/pentraxin 3 (HC–219 HA/PTX3) is considered in vivo to stimulate host regeneration of damaged tissues and to have regenerative potential for many clinical applications. However, it remains to be determined which specific factors are most critical for muscle regeneration. This knowledge could be useful for development of novel therapeutics specifically for VML defect healing.

This study is not without limitations. Although amniotic scaffold group muscle appears polarized and organized, its function was not specifically evaluated. Future studies will include gait analysis, maximum tetanic force generation, and muscle recruitment percentage to quantify functional muscle regeneration and synapse staining to evaluate reinnervation. Additionally, the model used in this study includes relatively small defects in young mice. As a step toward clinical translation, it will be important to understand the impact of defect size on scaled-up large animal studies. Although amniotic tissue products have been shown to be cost-effective for diabetic foot ulcers, cost analysis will be required to justify amniotic tissue product's high up-front cost. Finally, measurements were performed by a trained research fellow who was not blinded, which could have introduced bias. The amniotic scaffold group had greater variance in mCT and MRI measurements than the other groups. It is unclear whether this is due to measurement bias, variable host response, or variability in the product composition.

The results of this study demonstrate that an amniotic scaffold can improve muscle regeneration compared with collagen scaffold treatment or no treatment. Furthermore, amniotic scaffold reduced fibrosis and induced formation of organized muscle through its growth factors and cytokines.[27–29]

CONCLUSIONS

AMS may have the ability to promote muscle regeneration by exerting a paracrine effect on the host to regenerate polarized, structural muscle. This study serves as a proof of concept that AMS may be a promising, clinically feasible strategy that deserves further investigation for the treatment of VML defects.

Anand R. Kumar, MD
Department of Plastic Surgery
University Hospitals-Case Western Reserve University
11100 Euclid Ave Ste 1200
Cleveland, OH 44106
E-mail: anand.kumar@uhhospitals.org

REFERENCES

1. Grogan BF, Hsu JR; Skeletal Trauma Research Consortium. Volumetric muscle loss. *J Am Acad Orthop Surg.* 2011;19(suppl 1):S35–S37.
2. Garg K, Ward CL, Hurtgen BJ, et al. Volumetric muscle loss: persistent functional deficits beyond frank loss of tissue. *J Orthop Res.* 2015;33:40–46.
3. Kesireddy V. Evaluation of adipose-derived stem cells for tissue-engineered muscle repair construct-mediated repair of a murine model of volumetric muscle loss injury. *Int J Nanomedicine.* 2016;11:1461–1473.
4. Quarta M, Cromie M, Chacon R, et al. Bioengineered constructs combined with exercise enhance stem cell-mediated treatment of volumetric muscle loss. *Nat Commun.* 2017;8:15613.
5. Juhas M, Ye J, Bursac N. Design, evaluation, and application of engineered skeletal muscle. *Methods.* 2016;99:81–90.
6. Koffler J, Kaufman-Francis K, Shandalov Y, et al. Improved vascular organization enhances functional integration of engineered skeletal muscle grafts. *Proc Natl Acad Sci U S A.* 2011;108:14789–14794.
7. Levenberg S, Rouwkema J, Macdonald M, et al. Engineering vascularized skeletal muscle tissue. *Nat Biotechnol.* 2005;23:879–884.
8. Zelen CM, Serena TE, Denoziere G, et al. A prospective randomised comparative parallel study of amniotic membrane wound graft in the management of diabetic foot ulcers. *Int Wound J.* 2013;10:502–507.
9. Zelen CM, Serena TE, Snyder RJ. A prospective, randomised comparative study of weekly versus biweekly application of dehydrated human amnion/chorion membrane allograft in the management of diabetic foot ulcers. *Int Wound J.* 2014;11:122–128.
10. Penny H, Rifkah M, Weaver A, et al. Dehydrated human amnion/chorion tissue in difficult-to-heal DFUs: a case series. *J Wound Care.* 2015;24:104–109.
11. Zelen CM, Gould L, Serena TE, et al. A prospective, randomised, controlled, multi-centre comparative effectiveness study of healing using dehydrated human amnion/chorion membrane allograft, bioengineered skin substitute or standard of care for treatment of chronic lower extremity diabetic ulcers. *Int Wound J.* 2015;12:724–732.
12. Serena TE, Carter MJ, Le LT, et al; EpiFix VLU Study Group. A multicenter, randomized, controlled clinical trial evaluating the use of dehydrated human amnion/chorion membrane allografts and multilayer compression therapy vs. multilayer compression therapy alone in the treatment of venous leg ulcers. *Wound Repair Regen.* 2014;22:688–693.
13. Hu Y, Rao SS, Wang ZX, et al. Exosomes from human umbilical cord blood accelerate cutaneous wound healing through miR-21-3p-mediated promotion of angiogenesis and fibroblast function. *Theranostics.* 2018;8:169–184.
14. Han Y, Sun T, Han Y, et al. Human umbilical cord mesenchymal stem cells implantation accelerates cutaneous wound healing in diabetic rats via the Wnt signaling pathway. *Eur J Med Res.* 2019;24:10.
15. Cooke M, Tan EK, Mandrycky C, et al. Comparison of cryopreserved amniotic membrane and umbilical cord tissue with dehydrated amniotic membrane/chorion tissue. *J Wound Care.* 2014;23:465–474.
16. Röck T, Bartz-Schmidt KU, Landenberger J, et al. Amniotic membrane transplantation in reconstructive and regenerative ophthalmology. *Ann Transplant.* 2018;23:160–165. .
17. Tighe S, Moein HR, Chua L, et al. Topical cryopreserved amniotic membrane and umbilical cord eye drops promote re-epithelialization in a murine corneal abrasion model. *Invest Ophthalmol Vis Sci.* 2017;58:1586–1593.
18. Tang K, Wu J, Xiong Z, et al. Human acellular amniotic membrane: a potential osteoinductive biomaterial for bone regeneration. *J Biomater Appl.* 2018;32:754–764.
19. Demirkan F, Colakoglu N, Herek O, et al. The use of amniotic membrane in flexor tendon repair: an experimental model. *Arch Orthop Trauma Surg.* 2002;122:396–399.
20. Yang JJ, Jang E-C, Song K, et al. The effect of amniotic membrane transplantation on tendon-healing in a rabbit Achilles tendon model. *Tissue Eng Regen Med.* 2010;7:323–329.

21. Koizumi NJ, Inatomi TJ, Sotozono CJ, et al. Growth factor mRNA and protein in preserved human amniotic membrane. *Curr Eye Res.* 2000;20:173–177.

22. López-Valladares MJ, Teresa Rodríguez-Ares M, Touriño R, et al. Donor age and gestational age influence on growth factor levels in human amniotic membrane. *Acta Ophthalmol.* 2010;88:e211–e216.

23. Bańkowski E. Collagen of the umbilical cord and its alteration in EPH-gestosis (preeclampsia). *Proc Indian Acad Sci-Chem Sci.* 1999;111:207–213.

24. Jadalannagari S, Converse G, McFall C, et al. Decellularized Wharton's jelly from human umbilical cord as a novel 3D scaffolding material for tissue engineering applications. *PLoS One.* 2017;12:e0172098.

25. Sobolewski K, Małkowski A, Bańkowski E, et al. Wharton's jelly as a reservoir of peptide growth factors. *Placenta.* 2005;26:747–752.

26. Wang HD, Lough DM, Kurlander DE, et al. Muscle-derived stem cell-enriched scaffolds are capable of enhanced healing of a murine volumetric muscle loss defect. *Plast Reconstr Surg.* 2019;143:329e–339e.

27. Tighe S, Mead OG, Lee A, et al. Basic science review of birth tissue uses in ophthalmology. *Taiwan J Ophthalmol.* 2020;10:3–12.

28. Carter MJ. Dehydrated human amnion and chorion allograft versus standard of care alone in treatment of Wagner 1 diabetic foot ulcers: a trial-based health economics study. *J Med Econ.* 2020;23:1273–1283.

29. Niknejad H, Peirovi H, Jorjani M, et al. Properties of the amniotic membrane for potential use in tissue engineering. *Eur Cell Mater.* 2008;15:88–99.